Tracking and kinematical characterization of CME events in 3D using a supervised texture-based technique combined with automatic tie-point triangulation

Guillermo Stenborg[1], Carlos Braga[2], and Alisson Dal Lago[2]

[1] George Mason University (GMU), Fairfax, VA 22030; [2] National institute for Space Research (INPE), Sao Jose dos Campos SP, Brazil

Solar Information Processing Workshop VII

(August 18 - 21, 2014 — La Roche-en-Ardenne, Belgium)

Abstract

The identification of Coronal Mass Ejections events (CME) in white-light coronagraph images can simply be addressed as a bi-partitioning segmentation problem. Goussies et al., 2010a, 2010b showed that the overall spatial relationship of the gray levels (i.e., the texture) can be used as a discriminant to separate the CME feature from the background. As defined, the texture content is given by the relative probabilities that two neighboring pixels separated by a certain distance have specific gray levels. Their study allowed them to design a supervised technique to detect and track coronal events by means of their texture on a coronagraph field of view (a.k.a. *CORSET*: CORonal SEgmentation Technique). Later, to contribute to the implementation of a pseudo-automatic tool to unambiguously characterize the CME events, Braga et al., 2013 extended the capabilities of *CORSET* by adding new routines to determine several morphological and kinematical parameters (as projected onto the plane of the sky) without human intervention. Nowadays, with the advent of multiple white-light imagery at vantage observing points in space along with the development of customized 3D reconstruction techniques, the solar community can infer the real shape and direction of propagation of CME events (of utmost importance for space weather purposes). In this work, we took advantage of one particular 3D reconstruction tool (*Sunloop*, Liever et al., 2009, 2011) to derive the "true" kinematics of CMEs pseudo-automatically. *Sunloop* uses manually-defined tie points to derive the 3D localization of the apex of the event via triangulation. Such approach can be tedious if the user aims to de-project the leading edge (LE) of the CME feature on each frame. To make the procedure faster and more objective, we combined *Sunloop* and *CORSET*. In this way, the tie-points used to delimit the LE of the event on the different frames are generated fully automatically. The *CORSET-3D* technique does not have any geometric constraint, and hence CME features of practically any shape can be reconstructed. In this presentation, we briefly describe the technique and show a sample of the results obtained after applying it to a few Earth-directed CMEs observed by the COR2 coronagraphs on both SECCHI A and SECCHI B S/C between 2008 and 2011. In particular, we reconstructed the LE of the CMEs as a function of time and derived the "true" velocity and direction of propagation of the apex. Our findings are put in context with previous results.

The Technique: CORSET + Sunloop

CME tracking with CORSET: Brief Overview

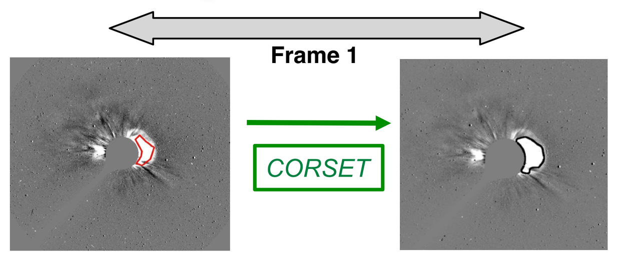

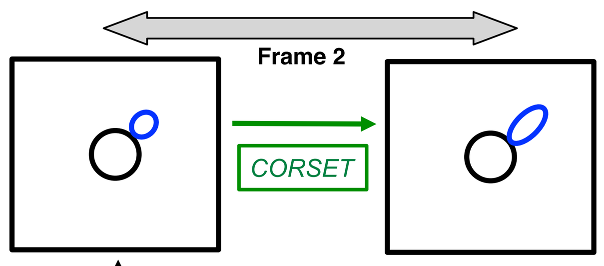

Base Diference Image

ROI: Foreground (CME) defined by the User

ROI: Segmentation obtained

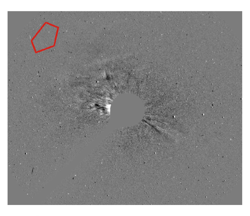

ROI: Background defined by the User

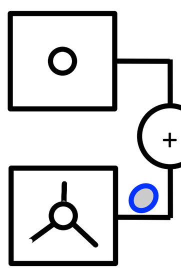

Data Input: Preprocessing caveats

- Background ratio images
  . Poor contrast, especially for faint events
  . Leading edge underestimated
- Base differences
  . The further a given frame from the base, the noticeable the streamer deflections (if any) ==> false detections
- Running differences
  . Inner region, artifacts introduced by previous stage of the event.
  . Inner region keeps changing as event develops altering its texture, and therefore losing the original meaning of tracking events by texture.

- CME detection objective addressed as a bipartitioning segmentation problem via front evolution using levels sets (Shi and Karl, 2006)

GLCM: Gray Level Co-occurrence Matrix

- (1) found that GLCM for the CME features does not follow exactly a known probability density function ==> Shi and Karl 2006, not applicable directly. (1) Goussies et al., 2010a, 2010b.

- (1) introduced a χ^2 statistical test to overcome the absence of a known probability density function and thus evaluate whether the two sets have the same distribution up to a certain level of significance (i.e., to determine whether the GLCM of a given pixel **x** , i.e., its texture, resembles that of the background or the foreground).

- To account for varying texture during development, re-evaluation of GLCM in expanded region in frame i+1 (Z/Q pixels in all directions, Z=size of segmented region in frame I, Q user-define). Q: tunable parameter (among others).

Data input: Preprocessing chosen

$$K_j(x,y)=\begin{cases} I_1(x,y)-I_{base}(x,y) & \text{if } j=1 \\ I_j(x,y)-I_{base}(x,y) & \text{if } j>1 \text{ and } (x,y)\in R_{j-1} \\ I_j(x,y)-I_{j-n}(x,y) & \text{if } j>1 \text{ and } (x,y)\notin R_{j-1} \end{cases}$$

Versatility

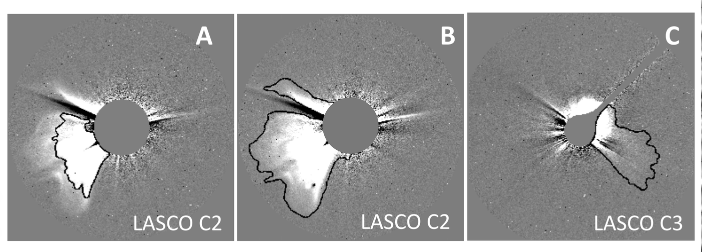

By choosing the appropriate set of tuning parameters, CORSET is able to track CME events without including the associated shock, if any (panel A), or b) including it (panel B), and even to discriminate between co-occurrent events (within certain limits, panel C).

CME leading edge tracking with CORSET + Sunloop

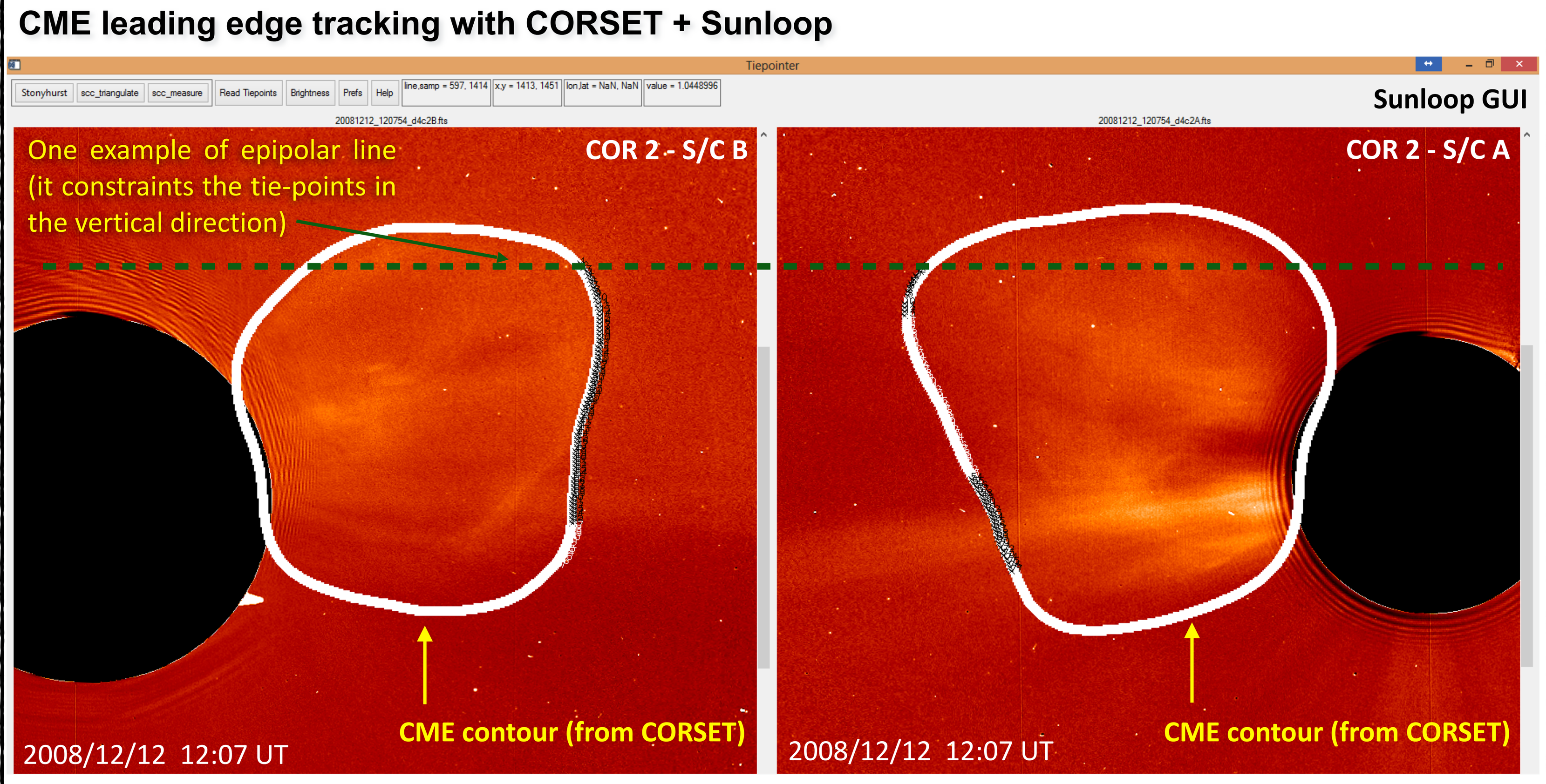

***Figure 1**: Sunloop (Liewer et al., 2009, 2011) is available as part of the Solar Soft SECCHI software library (e.g., http://www.lmsal.com/solarsoft/). The image is a screen dump of the "Sunloop/Tiepointer" tool showing the placement of automatic tie-points (black and white crosses on the CME leading edge contour). The white line shows the contour previously derived using CORSET (we modified the Sunloop code to allow the inclusion of the contours and the automatic determination of the tie points to be used for 3D reconstruction).*

- An epipolar line constraints the tie-point in one dimension of the image. Hence, once a tie-point is defined in a given view, the corresponding tie-point in the other view is free (along the epipolar line) and needs to be defined by the user. The exactly same feature must be selected in each image of the pair by visual inspection.
- In this work, on the other hand, we suppose that each tie-point of the CME LE contour (as defined by *CORSET*) in a given view corresponds to a tie-point in the corresponding image pair, which is defined by the intersection of the CME LE contour in this image pair and the corresponding epipolar line.
- Typically, the algorithm defines automatically from 50 to 200 tie-points in each COR2 image (2048x2048). We observed that the tie-points close to the lateral side of the CME produced inconsistent results, probably because they do not point to the same CME feature. For this reason we arbitrarily decided to remove 10% of the tie-points to each side of the CME, leaving the 80% tie-points in the central range unchanged.
- Once the set of matching tie-points pairs are defined in this automatic way, the *Sunloop* code calls the SolarSoft routine *ssc_triangulate* to perform the triangulation.

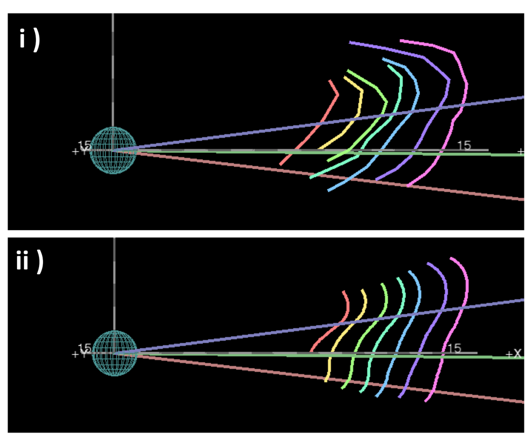

***Figure 2:** Time evolution of the 3D leading edge (the 7 colored lines) of the CME recorded by the COR 2 instruments on board the STEREO S/C on 2008/12/12 between 10:07:00 UT and 13:07:00 UT. The 3D reconstruction was generated with the "Sunloop" software using tie-points defined i) manually (top panel), and ii) by CORSET (bottom panel). The Sun is represented by the 3D globe. The three colored lines depict the directions to STEREO B (violet), Earth (green), and STEREO A (red). The picture was made using the "Animator" tool, which is part of the "Sunloop" software.*

Note in the top panel the non-smoothness of the contours derived and the unevenness of the spacing between contours, which speaks of the difficulty experienced by the observer to determine the outermost part of the event.

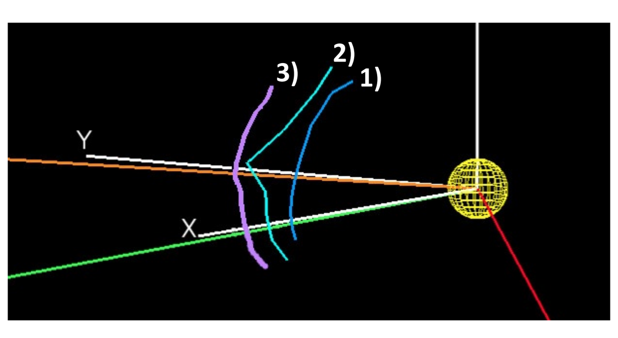

***Figure 3:** 3D CME leading edge contour of a test case event as determined with the "Sunloop" software using tie-points defined by 1) User #1 (blue); 2) User #2 (cyan); 3) CORSET (purple). The Sun is represented by the 3D globe. The three colored lines depict the directions to STEREO B (brown), Earth (green), and STEREO A (red). The picture was made using the "Animator" tool, which is part of the "Sunloop" software.*

Note the discrepancy between the results derived from the manual measurements of the same event performed by two independent observers (high degree of subjectivity).

CME Events Sample

Event #1: Earth-directed CME on 2010/04/03. Source at S25°W03°. S/C separation: ~139 deg.

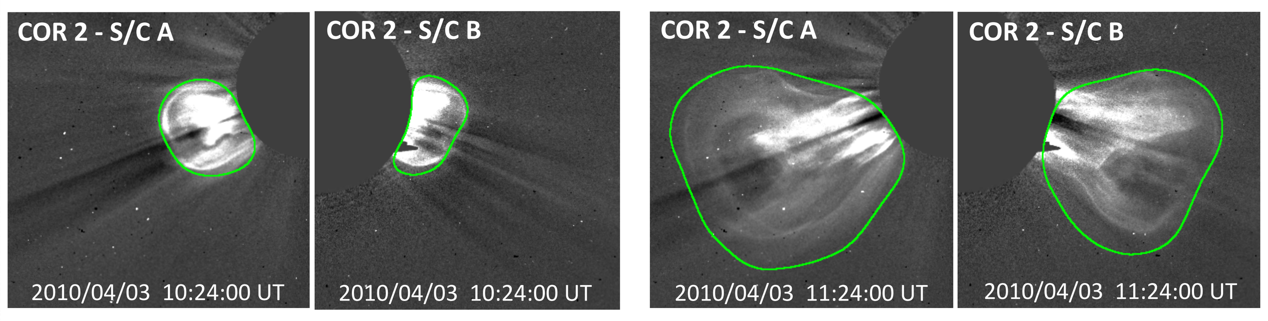

***Figure 4:** Sample frames showing CME segmentation on SECCHI/COR 2 coronagraphs using CORSET.*

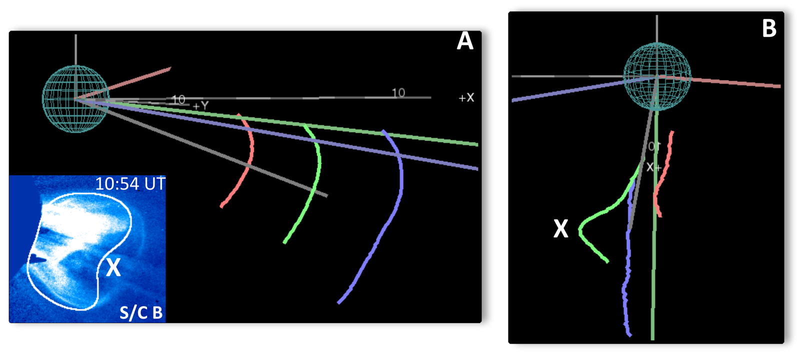

***Figure 5:** 3D evolution of CME LE as seen from two different viewpoints: A) a lateral view , i.e., 90 deg from Sun-Earth line, and B) a view from Earth (w/ "Sunloop/Animator" tool).*

Note the bulge on the green contour (X). It is due to an incorrect determination (by CORSET) of the CME LE in the corresponding frame.

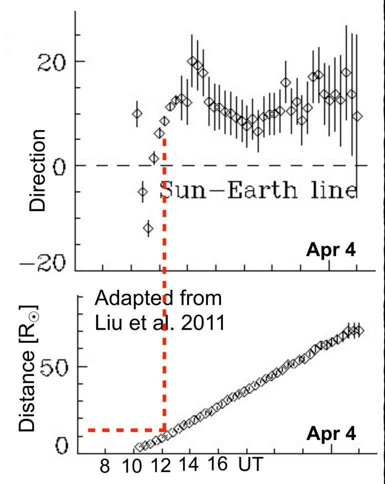

***Figure 6:** In this case, CORSET was run only for distances below 12 R☉ (see red dashed line); which might explain the discrepancy in longitude determined by CORSET.*

HEEQ: Heliocentric Earth Equatorial

	COR2 A Speed	COR2 B Speed	3D Speed (V)	Direction of Propagation (Heliocentric longitude HEEQ)
Liu et al. 2011	-	-	[800-1000] km/s (function of time)	[<10°, ecliptic plane] (Triangulation) See Fig. 6
Colaninno 2012	809 km/s (linear)	800 km/s (linear)	917 km/s (linear)	6° **CPA** (GCS model at 10 R☉)
Möstl et al. 2014	-	-	829 km/s (linear)	4° **CPA** (GCS model, average between 2.5 and 16.5 R☉)
This Work	822 km/s (PA 100°)	895 km/s (PA 253°)	865 km/s (linear)	-6° **Apex** (Triangulation < 12 R☉)

Event #2: Earth-directed CME on 2010/05/24. Source at N18°W26°. S/C separation: ~142 deg.

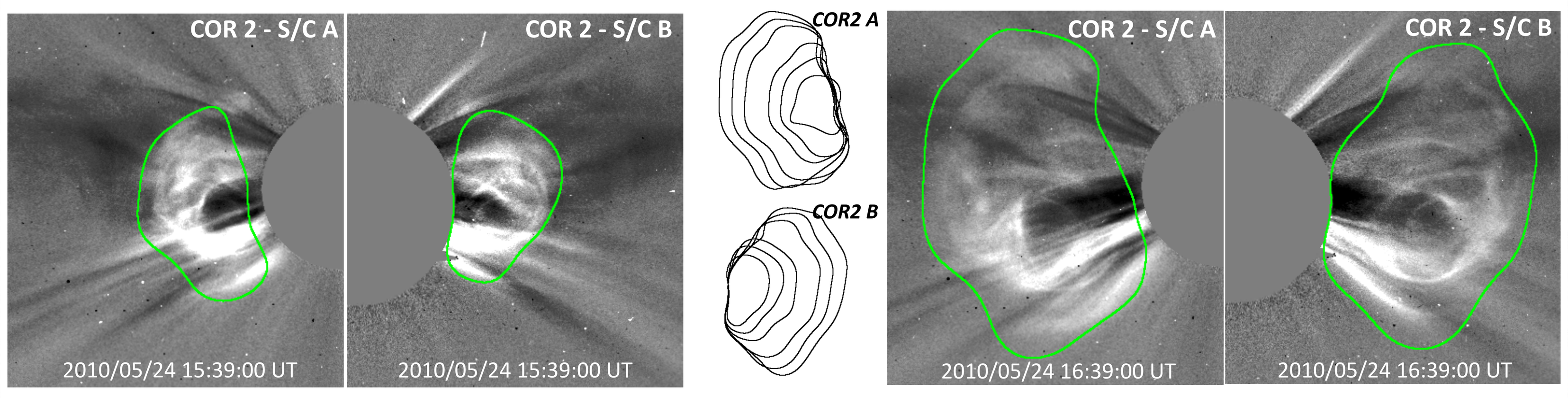

***Figure 7:** Sample frames showing CME segmentation on SECCHI/COR 2 coronagraphs using CORSET. The portion of the CME missed close to the limb is due to the pre-existent event partly superposed in the LOS on the base image used. In the middle, CORSET contours at ~~15:24~~, 15:39, 15:54, 16:24, 16:39, and 16:54 UT (COR2 A on top, B on bottom). Frame at 15.24 UT not used for 3D reconstruction.*

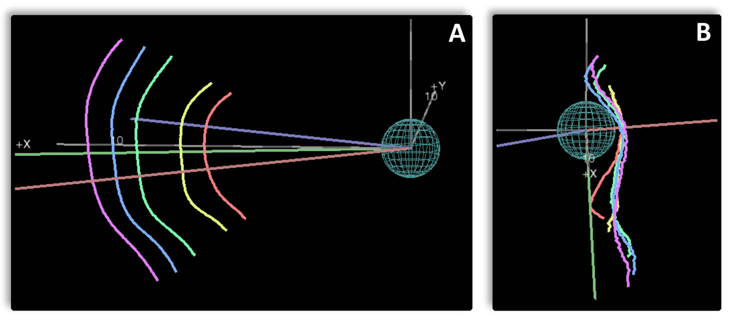

Warning

All 3D speeds determined in this work with CORSET correspond to the average speed of the fastest point of the CME LE (what we call its "Apex"), which not necessarily lies at the CME Central Position Angle (CPA).

***Figure 8:** 3D evolution of CME LE as seen from two different viewpoints: A) a lateral view , i.e., 90 deg from Sun-Earth line, and B) a view from Earth (w/"Sunloop/Animator" tool).*

	COR2 A Speed	COR2 B Speed	3D Speed (V)	Direction of Propagation (Heliocentric longitude HEEQ)
Lugaz et al. 2012	650 km/s (PA 95°)	650 km/s (PA 270°)	[500-700] km/s (function of time)	26° **CPA** (GCS, 9.5 R☉) /~11° (HI1, [18-20] UT, Triang.)
This Work	765 km/s (PA 70°)	645 km/s (PA 280°)	620 km/s (linear)	6° **Apex** (Triangulation < 12 R☉)

Event #3: Earth-directed CME on 2010/08/01. Source at N20°E35°. S/C separation:

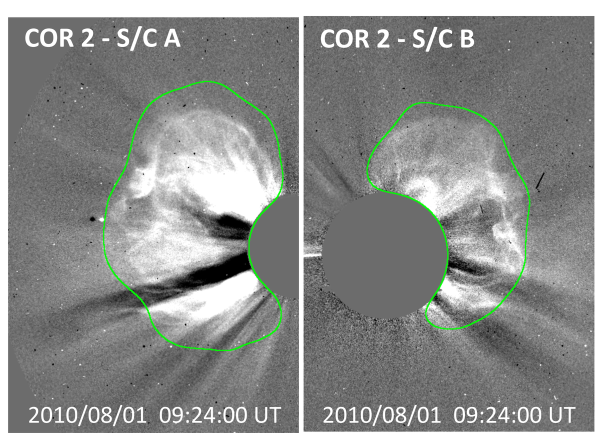

***Figure 9:** Sample frames showing CME segmentation on SECCHI/COR 2 coronagraphs using CORSET.*

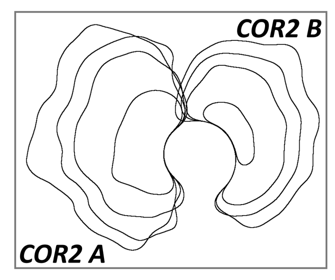

CORSET contours (08:54 - 09:24 - 09:39 - 09.54 UT)

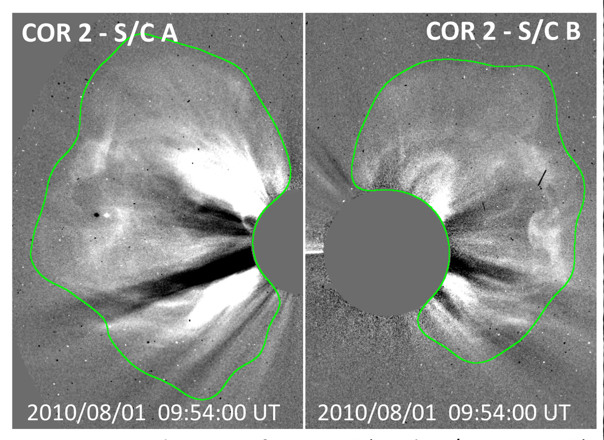

Note: COR2B data gap after 10 UT (until 08/02 04:00 UT).

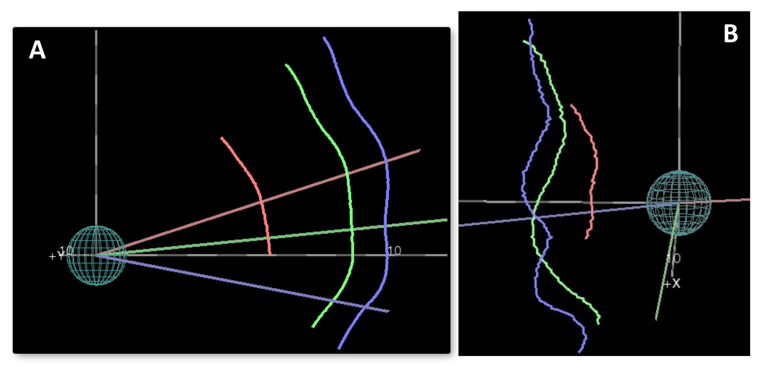

***Figure 10:** 3D evolution of CME LE as seen from two different viewpoints: A) and B) as in figures 5 and 8.*

	COR2 A Speed	COR2 B Speed
This Work	1279 km/s (PA 91°)	1390 km/s (PA 320°)

	3D Speed (V)	Direction of Propagation (HEEQ)
Liu et al. 2012	1140 km/s (linear)	[-24,-16°] **CPA** (Tri., [08:30-10] UT)
Temmer et al. 2012	1160 km/s (linear)	-28° **CPA** (GCS in COR1 & 2)
Temmer et al. 2012	1138 km/s (linear)	-20° **CPA** (Triang. in COR1 & 2)
This Work	1296 km/s (linear)	-24° **Apex** (Triangulation < 12 R☉)

Summary and Conclusions

- To contribute to a user-independent determination of the 3D kinematics of CME events, we have integrated i) a supervised texture-based technique to identify and track CME events on a coronagraph FOV (CORSET) into ii) an existing code aimed at determining manually the 3D location (and kinematics) of the CME leading edge via triangulation of tie-points (Sunloop). We named the technique CORSET-3D.
- The resulting method does not depend on visual inspection for tie-point identification and hence allows the 3D reconstruction of the time evolution of the whole CME leading edge in an objective way.
- We have shown some basic results obtained from applying CORSET-3D on a selected sample of 3 (earth-directed) CME events observed simultaneously by the SECCHI COR2 coronagraphs on both STEREO S/C A and B to reconstruct their 3D leading edge. We determined, in particular, both the direction of propagation of the CME apex and its "true" speed during their development throughout the inner corona (i.e., < ~15 R☉). Namely, we have shown in this poster the analysis for the CME events on:
  - 2010/04/03 [09:54 UT - 11:24 UT]; S/C separation ~139° (Liu et al., 2011; Colaninno 2012, Möstl et al., 2014)
  - 2010/05/24 [15:24 UT - 16:59 UT]; S/C separation ~142° (Lugaz et al., 2012)
  - 2010/08/01 [08:54 UT - 09:54 UT]; S/C separation ~150° (Liu et al. 2012; Temmer et al., 2012; also Harrison et.al., 2012)
- CORSET results reported here (i.e., speed and direction of propagation) were computed on the fastest moving point of the CME LE (i.e., its apex), while the corresponding results from previous works were obtained from the point in the LE at the Central Position Angle (CPA) of the CME (using same and/or different 3D reconstruction methods). In spite of this, we note that the difference in the direction of propagation (longitude) of the corresponding events computed using different methodologies (forward modeling vs triangulation) is within the error expected for the CGS model (i.e., ~10°) . Mierla et al. (2007) compared several methodologies for 3D reconstruction. In particular, they analyzed a set of 7 CME events and found a difference in the direction of propagation of up to 10° among the different methods. We therefore may conclude that for the sample shown in this work, CORSET-3D results are in agreement (within the expected error) with those from previous works.
- CORSET has now been adapted to work also on STEREO/SECCHI HI 1 images with promising results. A comprehensive analysis including more than 15 events (and considering other points along the LE for better comparison) is underway.
- In summary, CORSET capabilities (i.e., i) CME detection and tracking, and ii) automatic determination of kinematical and morphological parameters extracted from segmentation) combined with the Sunloop tool (3D reconstruction by triangulation using tie-points) is another step towards a more objective 3D characterization of CME events.

Acknowledgments

C. R. Braga thanks to CAPES and FAPESP (2008/08840-0 and 2012/05436-9) for financial support. A. Dal Lago thanks CNPq (grant 305351/2011-7). The STEREO/SECCHI data used here are produced by an international consortium of the Naval Research Laboratory (USA), Lockheed–Martin Solar and Astrophysics Lab(USA),NASA Goddard Space Flight Center (USA), Rutherford Appleton Laboratory (UK), University of Birmingham (UK), Max-Planck-Institutfür Sonnensystemforschung (Germany), Center Spatiale de Liege (Belgium), Institut d'Optique Theórique et Appliqueé (France), Institut d'Astrophysique Spatiale (France).

References

Braga, C.R.; Dal Lago A.; Stenborg, G.: *Adv. Sp. Res.* **51**,1949, 2013.

Colaninno, R. C.: *Ph.D. Thesis*, *George Mason Univeristy,* 2012. —- Colaninno, R. C.; Vourlidas, A.; Wu, C. C.: *JGR* **118**, 6866, 2013.

Goussies, Mejail, Jacobo, and Stenborg: Pattern Recognition Letters **31**, 496, 2010a. —— Goussies, N.; Stenborg, G.; Vourlidas, A.; Howard, R.: *Sol. Phys.* **262**, 481, 2010b.

Harrison, R.A.; Davies, J.; Möstl, C.; Liu, Y.; et al.: *ApJ* **750**, id.45, 2012.

Liewer, P.C.; De Jong, E.M.; Hall, J.R.; Howard, R.A.; Thompson, W.T.; Culhane, J.L.; Bone, L.A.; Van Driel-Gesztelyi, L.: *Sol. Phys.* **256**, 57, 2009.

Liewer P.C.; Hall J.R.; Howard R.A.; De Jong E.M.; Thompson W.T.; Thernisien A.: *JASTP* **73**, 1173, 2011.

Liu, Y.; Luhmann, J.G.; Bale, S.D.; Lin, R.P.: *ApJ* **734**, Id.84, 2011.

Liu, Y..; Luhmann, J.G.; Möstl, C.; Martinez-Oliveros, J.C.; Bale, S.D.; Lin, R.P.; Harrison, R.A.; Temmer, M.; et al.: *ApJ Letters* **746**, L15, 2012.

Lugaz, N.; Farrugia, C. J.; Davies, J. A.; Möstl, C.; Davis, C. J.; Roussev, I. I.; Temmer, M.: *ApJ* **759**, id.68, 2012.

Möstl, C.; Amla, K.; Hall, J. R.; Liewer, P. C.; De Jong, E. M.; Colaninno, R. C.; Veronig, A. M.; Rollett, T.; et al.: *ApJ* **787**, id.119, 2014.

Temmer, M.; Vrsnak, B.; Rollett, T., et al.: *ApJ* **749**, id.57, 2012.

Thernisien, A.; Howard R.; and Vourlidas, A.:, *ApJ* **652**, 763, 2006. —— Thernisien, A.; Vourlidas, A., and Howard, R., *Solar Phys.* **256**, 111, 2009..

Thernisien, A.: *ApJ Suppl. Ser.* 194, 33, 2011.